Journal of Membrane Science 574 (2019) 24–32

Contents lists available at ScienceDirect

Journal of Membrane Science

journal homepage: www.elsevier.com/locate/memsci

Water content, relative permittivity, and ion sorption properties of polymers for membrane desalination

Kevin Chang, Hongxi Luo, Geoffrey M. Geise*

Department of Chemical Engineering, University of Virginia, 102 Engineers' Way, P.O. Box 400741, Charlottesville, VA 22904, USA

ARTICLE INFO

Keywords:
Permittivity
Ion sorption
Dielectric
Polymer
Desalination

ABSTRACT

The interplay of polymer water content, dielectric relative permittivity, and ion sorption properties was studied using a cross-linked poly(glycidyl methacrylate) (XL-pGMA) polymer. The water content of the base XL-pGMA polymer was increased, by partial hydrolysis of the epoxide ring on the polymer side chain, to prepare a series of hydrolyzed XL-pGMA materials. Microwave dielectric spectroscopy, performed from 45 MHz to 26.5 GHz, revealed lower relative permittivity at a given water content compared to Nafion® 117. This observation suggests that knowledge of polymer water content alone may be insufficient for estimating relative permittivity properties of hydrated polymers. State of water analysis suggested that (for polymers that contain similar total amounts of sorbed water) more water in hydrolyzed XL-pGMA interacts with the polymer compared to that in Nafion® 117, and this result may be related to the observed differences in the relative permittivity properties of the two materials. The hydrolyzed polymers were more water/ion sorption selective, important for desalination applications, compared to many uncharged materials reported in the literature but less selective compared to Nafion® 117. Membrane phase mean ionic activity coefficients suggest that Nafion® 117 is more thermodynamically ideal (i.e., the mean ionic activity coefficients are closer to unity) than the hydrolyzed XL-pGMA materials, and thus, ion exclusion in Nafion® 117 is primarily due to Donnan exclusion. Measured static relative permittivity values were used to estimate, via electrostatic theory, the free energy barrier for ion sorption in each material, and these values were qualitatively consistent with values determined using measured ion sorption data. This study suggests that polymer chemistry, not water content alone, influences the relative permittivity properties of hydrated polymers and that relative permittivity measurements can provide qualitative insight into ion sorption properties, which is important for designing advanced desalination membranes.

1. Introduction

Polymers are widely used as membranes to efficiently desalinate saline water and address global water shortages [1–7]. Commercially available desalination membranes, however, are susceptible to degradation via chlorine-based compounds used to disinfect water, so advanced chemically-stable desalination membranes are needed to address this challenge [8–10]. To be effective, these membranes must prevent ions (or salt) from passing through the membrane [11,12].

One approach to designing effective desalination membranes is to prepare membrane materials that suppress ion sorption (i.e., make thermodynamic partitioning of ions into the membrane from the external solution unfavorable) [4,13,14]. Reducing ion sorption in polymer membrane materials can lead to favorable salt rejection properties and efficient desalination [5]. Therefore, it is important to understand how to engineer polymer chemistry to suppress ion sorption and maximize the desalination performance of membranes.

Many theories that relate ion sorption properties to polymer properties seek to describe the free energy change associated with moving an ion from solution into the membrane phase and require knowledge of the relative permittivity (or static dielectric constant) [15] of the hydrated polymer [13,16–22]. One challenge facing the use of these theories is that few investigators have reported relative permittivity data for hydrated polymers of interest for desalination membrane applications. Relative permittivity data have been reported for Nafion® 117 [23–26], sulfonated polysulfone [26], uncharged hydrogels [27,28], cellulose acetate [29], polyamide [30], and other polymers [31,32]. Only a few studies, however, investigated polymers over a range of water content and/or in the microwave frequency range, which is particularly relevant for hydrated polymers.

While the relative permittivity of a hydrated polymer is expected to increase with increasing polymer water content [23,24,33,34], the functional nature of this increase and its dependence on polymer chemistry is not well understood. Recent studies have estimated the

* Corresponding author.
E-mail address: geise@virginia.edu (G.M. Geise).

https://doi.org/10.1016/j.memsci.2018.12.048
Received 6 August 2018; Received in revised form 7 October 2018; Accepted 17 December 2018
Available online 18 December 2018
0376-7388/

relative permittivity (i.e., static dielectric constant) of hydrated polymers using Nafion® 117 data [13,21,22,35]. This estimation assumes that the relative permittivity varies linearly between the relative permittivity values for poly(tetrafluoroethane) (PTFE) and bulk water [13,36]. This approximation is supported by data for Nafion® [13] and liquid mixtures of water and dimethyl sulfoxide [37], but data for other liquid mixtures [38–40] suggest that a linear relationship between relative permittivity and water content may not be universally applicable to hydrated polymers.

Here we report an investigation of the relationship between hydrated polymer relative permittivity properties and water content in a series of polymers based on poly(glycidyl methacrylate) (pGMA) that was cross-linked using poly(propylene glycol) bis(2-aminopropyl ether). We increased the water content of these polymers by hydrolyzing the epoxide ring on the pGMA side chain to increasing extents. Results were compared to Nafion® 117, which is a perfluorosulfonic acid polymer widely considered for fuel cell applications [41] to investigate the influence of polymer chemistry on relative permittivity properties. While Nafion® 117 and the materials considered in this study are chemically different (Nafion® contains highly charged sulfonic acid groups and is not cross-linked), the comparison made in this study is important as very little microwave frequency dielectric permittivity data have been reported for hydrated polymers. Furthermore, the Nafion® data used for comparison in this study has been used to describe the dielectric permittivity properties of other hydrated polymers, so it is important to understand how chemical differences between polymers influence hydrated polymer dielectric permittivity properties.

Relative permittivity increased as the pGMA side chains were increasingly hydrolyzed and polymer water content increased. The functional form of the increase in the relative permittivity of the cross-linked hydrolyzed pGMA-based polymers considered in this study with increasing water content was different from that reported for Nafion® 117. These results suggest that polymer chemistry and/or structure, not water content alone, may play a significant role in determining the relative permittivity properties of hydrated polymers.

Furthermore, we measured and analyzed the ion sorption properties of the materials to evaluate the effectiveness of using relative permittivity measurements to understand the ion sorption properties of hydrated polymers. The free energy barrier for ion sorption in the hydrated polymer was calculated using measured relative permittivity values and electrostatic theory. These calculated values were qualitatively consistent with the measured data and suggest that measured relative permittivity data for hydrated polymers may provide qualitative insight into ion sorption properties. Therefore, controlling polymer relative permittivity via the chemical functionality of the polymer could be a viable strategy to prepare polymer membrane materials that effectively suppress ion sorption, and relative permittivity measurements made on hydrated polymers may provide insight into the design of future desalination membranes.

2. Materials and methods

2.1. Materials

Poly(glycidyl methacrylate), pGMA, was synthesized from glycidyl methacrylate (GMA, 97%, Sigma-Aldrich, St. Louis, MO) using a reported initiators for continuous activator regeneration atom transfer radical polymerization (ICAR ATRP) technique [42]. The weight-average molecular weight (M_w) and polydispersity index (PDI) of the resulting polymer were determined to be 24,000 g/mol and 1.11, respectively, via gel permeation chromatography (GPC) using tetrahydrofuran (THF) as the solvent and polystyrene as the molecular weight standard. The pGMA polymer was mixed with poly(propylene glycol) bis(2-aminopropyl ether) (Mn ~ 2000 g/mol, Sigma Aldrich, St. Louis, MO) cross-linker (such that the composition of cross-linker in the mixture was 2.4% by mole) and was dissolved in a 5:1 (by volume) solution of dimethyl sulfoxide (DMSO, ≥ 99.9%, Macron Fine Chemicals): *N*-methyl-2-pyrrolidone (NMP, laboratory grade, Fisher Chemical). The cross-linker content of 2.4% (by mole) balanced the need to prepare mechanically robust membranes that could be characterized via microwave dielectric spectroscopy with the goal of minimizing the amount of cross-linker to probe the influence of co-monomer functionality on the dielectric properties of the materials.

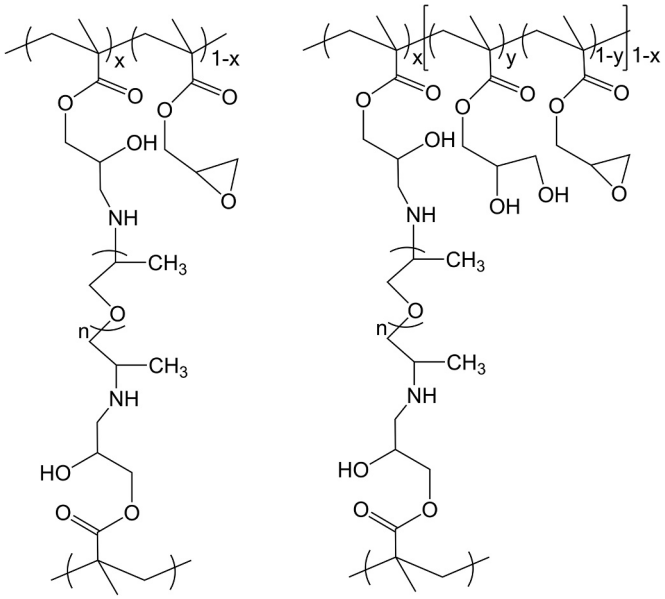

Fig. 1. Structures of non-hydrolyzed, i.e., XL-pGMA-0, (left) and partially hydrolyzed, i.e., XL-pGMA-z, (right) materials. The value of z in the sample nomenclature corresponds to the hydrolysis time (in hours) during the membrane preparation process, i.e. z is 0 for the non-hydrolyzed material, and z is 8, 10, or 12 for the partially hydrolyzed materials. All materials were prepared from a base polymer that contained 2.4% (by mole) cross-linker (i.e., x = 0.024), and the value of y increased as the hydrolysis time increased.

The casting solution (5.2% polymer and cross-linker in solvent, by mass) was poured into a flat PTFE mold and was heat treated to remove solvent, cross-link the polymer, and obtain a dense cross-linked pGMA membrane (XL-pGMA). Coupons of XL-pGMA were cut and subsequently immersed in 0.5 mol/L sulfuric acid (H_2SO_4) solution at 318 K for either 8, 10, or 12 h to partially hydrolyze the epoxide rings on the pGMA side chains (Fig. 1). The nomenclature for the hydrolyzed XL-pGMA materials is XL-pGMA-z where z represents the hours of hydrolysis used to prepare the material. Additional details about ICAR ATRP synthesis, membrane casting, and FT-IR characterization are provided in Supplementary information (SI).

The XL-pGMA-z materials were compared to PTFE (i.e., Teflon®) and Nafion® 117 polymers. PTFE was used as an uncharged, hydrophobic, and low dielectric loss control material [23,34,43]. Relative permittivity, differential scanning calorimetry (DSC), and ion sorption data for the XL-pGMA-z materials were compared to those data for Nafion® 117 (Alfa Aesar, catalog number 42180), a perfluorinated ionomer consisting of a hydrophobic PTFE backbone and side chains terminating with sulfonic acid groups. Prior to use, Nafion® samples were treated by boiling the samples in 3% hydrogen peroxide for one hour, rinsing the samples in boiling water for one hour, then boiling the samples in 0.5 mol/L H_2SO_4 for one hour, and finally, rinsing the samples in boiling water for one hour [23,34,44,45]. All samples were stored in de-ionized (DI) water (18.2 MΩ cm) until use.

2.2. Methods

2.2.1. Water uptake

The XL-pGMA-z and Nafion® 117 samples first were equilibrated in DI water for at least 48 h. Then, samples were removed from DI water,

excess surface water was quickly and thoroughly removed, and the wet sample mass, m_w, was measured. Samples subsequently were dried under vacuum in vented Petri dishes [46,47] at room temperature for at least 48 h. After drying, samples quickly were removed from the oven, and the dry sample mass, m_d, was measured. Water uptake, w_u, was calculated as:

$$w_u = \frac{m_w - m_d}{m_d} \tag{1}$$

The volume fraction of water sorbed in the polymer, ϕ_w, was calculated using the water uptake data assuming volume additivity of water and polymer [48,49]:

$$\phi_w = \frac{w_u}{w_u + \frac{\rho_w}{\rho_p}} \tag{2}$$

where ρ_w is the density of water (1.0 g/cm^3) [50], and ρ_p is the dry polymer density. Dry polymer density was measured using an Archimedes' principle method, where sample mass was measured in air, m_{air}, and in an auxiliary liquid, m_{aux} [49,51–53]. The dry polymer density was calculated as:

$$\rho_p = \frac{m_{air}}{m_{air} - m_{aux}}(\rho_{aux} - \rho_{air}) + \rho_{air} \tag{3}$$

where ρ_{aux} is the density of the auxiliary liquid, ρ_{air} is the density of air. Cyclohexane was used as the auxiliary solvent [49,51], and the measurement temperature was used to determine the density of cyclohexane [50,54]. The volume fraction of water sorbed in the polymer is effectively equal to the water sorption coefficient, K_w, that is used in the desalination membrane literature and is defined as the ratio of the concentration of water in the polymer to that in the bulk external solution [4,49,55].

2.2.2. Microwave dielectric spectroscopy

Dielectric permittivity properties of the samples were characterized as the frequency-dependent relative complex permittivity, ε^* [15,24], using a microwave dielectric spectroscopy technique developed by Nicolson, Ross, and Weir (NRW) [56,57]. The real part of the relative complex permittivity, ε', is typically referred to as simply the relative permittivity or the dielectric constant, and the imaginary part of the relative complex permittivity, ε'', is typically referred to as the dielectric loss [15].

Two port scattering parameter (S-parameter) measurements were made using a Keysight N9928A vector network analyzer (VNA). The data were analyzed using the Keysight N1500A materials measurement software. A 10 cm long and 3.5 mm diameter coaxial transmission line (Maury Microwave, catalog number 8043S10) was used as the sample holder, and shielded coaxial cables (Keysight Technologies, catalog number N9910X0–708) were used to connect the VNA to the transmission line. A full two-port calibration was performed to define the calibration reference plane using 3.5 mm short, open, and load impedance standards (Maury Microwave, catalog number 8050CK) and one transmission line standard (i.e., directly connecting the two coaxial cables together) [15,24,37,58].

Samples were exposed to electromagnetic radiation over a frequency range of 45 MHz to 26.5 GHz in the transmission line (or waveguide) sample holder. This frequency range was chosen because water molecules in the hydrated polymer are sensitive to electromagnetic radiation in the microwave region of the spectrum [23,24,26,34,37,59]. The amplitude and phase of the reflected and transmitted electromagnetic radiation was measured (in two directions) using the VNA and expressed as four S-parameters: S_{11}, S_{12}, S_{21}, and (Fig. S2) that describe the properties of the material under test. The S-parameters are related to the relative complex permittivity, ε^*, and relative complex permeability, μ^*, properties as [56,60–62]:

$$S_{21} = S_{12} = \frac{(e^{-j\frac{\omega}{c}\sqrt{\mu^*\varepsilon^*}d})\left[1-\left(\frac{\sqrt{\frac{\mu^*}{\varepsilon^*}}-1}{\sqrt{\frac{\mu^*}{\varepsilon^*}}+1}\right)^2\right]}{1-\left[\left(\frac{\sqrt{\frac{\mu^*}{\varepsilon^*}}-1}{\sqrt{\frac{\mu^*}{\varepsilon^*}}+1}\right)^2(e^{-j\frac{\omega}{c}\sqrt{\mu^*\varepsilon^*}d})^2\right]} \tag{4}$$

$$S_{11} = S_{22} = \frac{\left(\frac{\sqrt{\frac{\mu^*}{\varepsilon^*}}-1}{\sqrt{\frac{\mu^*}{\varepsilon^*}}+1}\right)\left[1-(e^{-j\frac{\omega}{c}\sqrt{\mu^*\varepsilon^*}d})^2\right]}{1-\left[\left(\frac{\sqrt{\frac{\mu^*}{\varepsilon^*}}-1}{\sqrt{\frac{\mu^*}{\varepsilon^*}}+1}\right)^2(e^{-j\frac{\omega}{c}\sqrt{\mu^*\varepsilon^*}d})^2\right]} \tag{5}$$

where ω is the angular frequency, c is the speed of light in vacuum, and d is the length dimension that describes how much of the transmission line is filled with sample (Fig. S2).

An algorithm, proposed by Bartley and Begley [60] and built into the analysis software [63], was used to calculate the relative complex permittivity properties of the samples. This algorithm is suitable for non-magnetic materials, and it reduces noise and mismatch errors during data analysis [60,63]. It also addresses known issues with the NWR technique such as an analysis issue where multiple ε^* and μ^* values can be calculated from a single set of S-parameters and a measurement issue at frequencies corresponding to situations where the sample length is an integer multiple of one-half wavelength [56,60,62].

Samples were loaded into the transmission line in a manner that minimized air gaps (i.e., the sample filled the annular space in the coaxial transmission line) as air gaps can introduce measurement artifacts. PTFE was machined to fit perfectly in the annular space of the transmission line, and XL-pGMA-z films were tightly wrapped around the inner conductor of the transmission line until sufficient polymer was wrapped to fill the annular space of the transmission line [34]. Measurements using DI water were performed by directly pipetting DI water into the vertically positioned transmission line fitted with a customized silicone dielectric plug at the bottom end to prevent leaks. The influence of the plug on the DI water measurements was taken to be negligible, which was consistent with previous studies [24,37,64–66].

2.2.3. State of water analysis

Differential scanning calorimetry (DSC, TA Instruments Q1000) was used to characterize the states of water present in DI water equilibrated XL-pGMA-z and Nafion® 117 samples. Each sample (masses ranged from 3 to 6 mg) was sealed in a hermetic aluminum pan to avoid water loss during the experiment. The samples were quenched to −70 °C, scanned once from –70 to 90 °C at a heating rate of 10 °C/min under a dry nitrogen purge [49,67].

2.2.4. Ion sorption

Ion sorption was measured using a desorption method [14]. Samples were initially equilibrated with 0.5 mol/L sodium chloride (NaCl) solution for at least 7 days, which was 28 times larger than the characteristic time for diffusion in these materials [49,68–70]. After equilibration, samples were removed from the NaCl solution, the residual surface solution was quickly and thoroughly removed, and the samples were placed in a known volume of DI water. The sorbed ions in the sample then desorbed from the polymer into the external solution. The ion sorption coefficient, K_s, (defined as the ratio of the ion, or salt, concentration in the polymer relative to the ion concentration of an external solution in equilibrium with the polymer [14]) was calculated as:

$$K_s = \frac{C_s^m}{C_s^s} = \frac{C_d V_d}{C_s^s V_p} \tag{6}$$

where C_s^m is the ion concentration in the membrane, C_s^s is the ion concentration in the initial external solution (i.e., 0.5 mol/L NaCl), C_d is the

Table 1
Water content and dry polymer density data measured at 295 ± 1 K. Water content measurements were made on samples initially equilibrated with DI water. The volume fraction of water in the polymer, ϕ_w, (equivalent to the water sorption coefficient, K_w) was calculated from water uptake and dry density data using Eq. (2) [4]. The uncertainty was taken as the standard deviation from the mean of three measurements. Hydrolysis time, z, refers to the length of time (in hours) that the XL-pGMA-z samples were immersed in 0.5 mol/L H_2SO_4 at 318 K.

Polymer	Hydrolysis Time, z (h)	Water Uptake [g(water)/ g(dry polymer)]	Dry Density (g/cm^3)	ϕ_w
XL-pGMA-z	0	0.036 ± 0.002	1.22 ± 0.02	0.042 ± 0.003
	8	0.163 ± 0.008	1.23 ± 0.01	0.167 ± 0.008
	10	0.238 ± 0.011	1.25 ± 0.01	0.229 ± 0.016
	12	0.308 ± 0.007	1.25 ± 0.01	0.278 ± 0.012
Nafion® 117	–	0.197 [71]	1.98 [72]	0.280

final ion concentration in the desorption solution, V_d is the desorption solution volume, and V_p is the volume of the hydrated sample. Because monovalent NaCl was used in these experiments, the concentrations of sodium, chloride, and salt in a given solution were equivalent.

3. Results and discussion

3.1. Water uptake

We controlled the water content of XL-pGMA by partially hydrolyzing the epoxide ring to determine the influence of polymer water content on the relative permittivity of the hydrated polymer. The water content of XL-pGMA-z increased as the hydrolysis time (z in units of hours) increased (i.e., as the hydroxyl group content of the polymer, or value of y in Fig. 1, increased) (Table 1). The hydrolysis process did not affect significantly the dry density of the polymer. The water sorption coefficient for Nafion® 117 was calculated using reported water uptake and dry density data [71,72].

3.2. Microwave dielectric spectroscopy

Following each calibration, we measured the dielectric properties of air in the empty transmission line to verify the calibration. The measured relative permittivity (i.e., static dielectric constant) of air was essentially constant, over the frequency range considered, at a value of 1.0014 (Fig. S3). This value is consistent with the reported value of 1.0006 [73].

The relative permittivity of PTFE was also measured to be essentially constant over the range of frequencies considered. The measured relative permittivity of 1.898 and dielectric loss of 0.008 at 9.95 GHz, are very similar to reported values (2.048 and 0.001, respectively, at 9.95 GHz) [24,43]. The lower experimental value compared to the reported value may result from small air gaps between the sample and the wall of the transmission line (perhaps due to imperfections in the machined PTFE sample) [71,73]. Such small air gaps would tend to reduce the relative permittivity.

The observation that the dielectric permittivity values for air and PTFE do not change significantly as a function of frequency (Fig. S3) is due to the absence of significant dipole relaxation mechanisms in air and PTFE [74]. Alternatively, dipole relaxations do occur in water. We measured the dielectric permittivity properties of DI water using different sample lengths (i.e., different values of d achieved by loading different volumes of water into the transmission line) to optimize the measurement (SI, Fig. S2) [75]. DI water relative permittivity and dielectric loss data were well represented by a single Debye relaxation process (SI Section S.3.2) in agreement with the literature [34,59,76].

Using the single Debye relaxation process model, the static permittivity, ε_s, and the relaxation peak position in the dielectric loss data for DI water were regressed to be 77.98 ± 0.09 and 20.6 ± 0.1 GHz, respectively [23,77]. These values are similar to reported values (80.18 and 18 GHz, respectively) [77]. The measured static permittivity (i.e., the relative permittivity value measured at the lowest frequency) was 79.15 at 45 MHz, which agrees better with the reported value compared to that determined using the single Debye relaxation model. The lower values obtained in our measurement/regression could result from the presence of small air bubbles in the DI water in the transmission line. Due to the metallic nature of the transmission line, it was difficult to determine whether bubbles were present.

The Debye relaxation process observed for water is different from the dielectric permittivity versus frequency behavior observed for air and PTFE. At sufficiently low frequencies, the alternating electric field is slow enough that the water dipoles are able to remain in phase with the field, and energy can be stored in the aligned dipoles [74]. As the frequency increases, energy begins to dissipate as the electric field oscillations become faster and exceed the rate at which water dipoles can align [74]. In this situation orientation polarization disappears, and water dipoles are no longer able to remain in phase with the external electric field [74]. Therefore, we observe a drop in relative permittivity and a relaxation peak in the dielectric loss data (Fig. S4) [74].

We expect the dielectric permittivity data for hydrated XL-pGMA-z to have features similar to that of both PTFE and water because the water content of XL-pGMA-z is between that of PTFE and water. The relative permittivity data for XL-pGMA-0 is similar to that of PTFE but higher in absolute value (Fig. 2A). This result is consistent with the low water content of XL-pGMA-0. As the water content of XL-pGMA-z increased (i.e., as z increases), we observed an increase in the magnitude of the relative permittivity, and the shape of the relative permittivity versus frequency data began to assume a shape more characteristic of water compared to PTFE. This result is reasonable given that increased water content means that more dipolar relaxations are possible in the polymer.

We compared the dielectric relative permittivity properties of XL-pGMA-z to that of Nafion® 117. The XL-pGMA-12 material has similar water content to Nafion® 117. The relative permittivity of XL-pGMA-12, however, is considerably lower (by approximately a factor of 5) compared to that for Nafion® 117 (Fig. 2A).

Similar to the DI water data, XL-pGMA-z data were fit to a single Debye relaxation process model to determine the static permittivity (i.e., static dielectric constant) of the hydrated polymer (Fig. 2B). The XL-pGMA-z static permittivity values increased as polymer water content increased, with values of 2.2, 3.9, 4.4, and 5.3 for XL-pGMA-0, −8, −10, and −12 samples, respectively. The data for XL-pGMA-0, −8, and −10 were described reasonably well by a single Debye relaxation. However, the XL-pGMA-12 data deviated more from the single Debye relaxation description compared to the other materials. This observation may indicate the existence of more than one relaxation mechanism in this material.

3.3. State of water analysis

We observed differences between the XL-pGMA-12 relative permittivity data and that for Nafion® 117. These materials have similar volume fractions of water, so chemical differences between the two

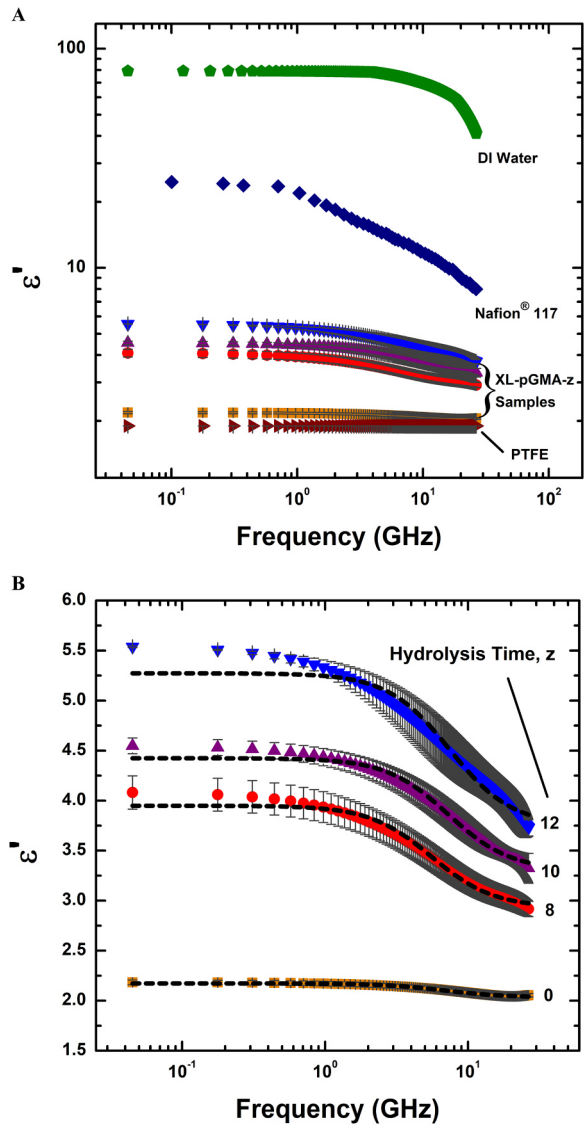

Fig. 2. (A) Relative permittivity, ε', as a function of frequency for DI water, Nafion® 117 [71], XL-pGMA-z, and PTFE. (B) Data for XL-pGMA-z are shown with the single Debye relaxation fit (dashed curves). The hydrolysis time, z, is labeled for each XL-pGMA-z sample. All measurements were made at 295 ± 1 K, and the uncertainty was taken as the standard deviation from the mean of three measurements.

materials appear to influence the relative permittivity properties. This difference may be linked to water dynamics, so we performed DSC measurements on hydrated XL-pGMA-z and Nafion® 117 to quantify the relative amounts of freezable (i.e., bulk, or weakly bound water) and non-freezable water (i.e., strongly bound water) in the polymers [33,41,78–84]. Both freezable, w_f, and non-freezable, w_{nf}, water content were calculated for XL-pGMA-z and Nafion® 117 as [80]:

$$w_f(\%) = \frac{m_f}{m_d}\times 100\% = \left[\frac{\Delta H_{polymer}}{\Delta H^{\circ}_{m,H_2O}} \times (w_u+1)\right]\times 100\% \quad (7)$$

$$w_{nf}(\%) = (w_u\times 100\%) - w_f(\%) \quad (8)$$

where m_f is the mass of freezable water in the polymer, $\Delta H_{polymer}$ is the enthalpy of melting (determined from the DSC thermogram) in the polymer, and $\Delta H^{\circ}_{m,H_2O}$ is the enthalpy of melting for water (333.5 J/g) [80].

We did not observe evidence of a melting transition at 0 °C for the XL-pGMA-0 material (Fig. 3). This result is reasonable given that very little water is absorbed by that polymer. As water content increased, we observed an increase in the intensity and breadth of the melting transitions observed at 0 °C, suggesting the presence of more freezable water in the partially hydrolyzed materials. The amounts of both freezable and non-freezable water increased as XL-pGMA-z hydrolysis time, z, increased (Table 2).

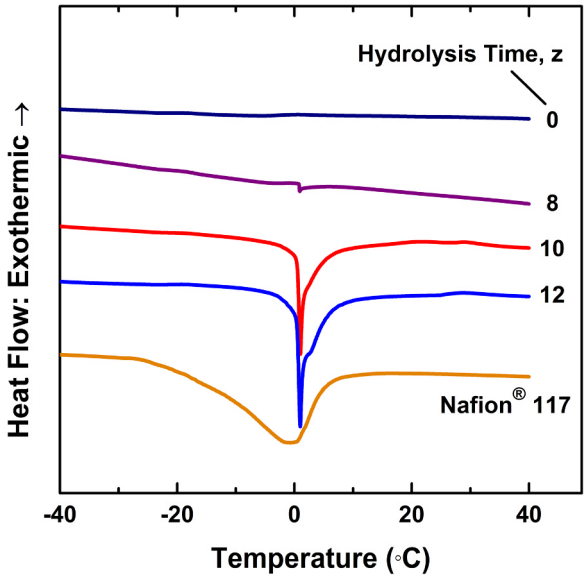

Fig. 3. Differential scanning calorimetry (DSC) thermograms for XL-pGMA-z and Nafion® 117. The hydrolysis time, z, refers to the length of time (in hours) that the XL-pGMA-z samples were immersed in 0.5 mol/L H_2SO_4 at 318 K.

Table 2
The distribution of freezable and non-freezable water in XL-pGMA-z samples and Nafion® 117. The values for XL-pGMA-z were calculated using water uptake data reported in Table 1. The values for Nafion® 117 were calculated using a measured water uptake of 0.320 ± 0.005 g(water)/g(dry polymer). This value was measured using Nafion® 117 films treated in the same manner as those films analyzed via DSC. The effect of residual water in Nafion® 117 after vacuum drying (as discussed in the literature) [85,86] was estimated to potentially affect the results by approximately 2%. The sum of the values of w_f and w_{nf} is equivalent to the total water uptake of the material (Eq. (8)). The hydrolysis time, z, refers to the length of time (in hours) that the XL-pGMA-z samples were immersed in 0.5 mol/L H_2SO_4 at 318 K.

Polymer	Hydrolysis Time, z (h)	w_f (%)	w_{nf} (%)
XL-pGMA-z	0	0.05	3.5
	8	0.3	16.1
	10	2.6	21.2
	12	4.1	26.8
Nafion®117	–	9.7	22.4

We observed a much broader melting transition for Nafion® 117 compared to XL-pGMA-12 (Fig. 3, both materials have comparable water content). The melting peak for Nafion® 117 suggests the presence of more freezable (i.e., bulk or weakly bound) water [34,87–90] compared to XL-pGMA-12. The XL-pGMA-12 material contained less freezable water than Nafion® 117 (4.1% compared to 9.7%) and more non-freezable water (26.8% compared to 22.4%) compared to Nafion® 117 (Table 2). Since the total water content of the two materials is similar, this result suggests that sorbed water in XL-pGMA-12 interacts with the polymer backbone (via hydrogen bonding interactions) to a greater extent compared to Nafion® 117. The higher relative permittivity of Nafion® 117 compared to XL-pGMA-12 (Fig. 2) likely results from the presence of more freezable water in Nafion® 117 compared to XL-pGMA-12.

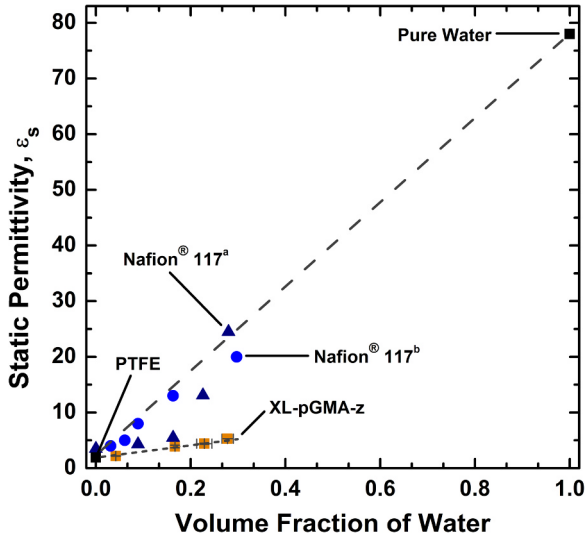

Fig. 4. Static permittivity, ε_s, of XL-pGMA-z (measured at 295 ± 1 K), Nafion® 117[a] (measured at 298 K) [71], and Nafion® 117[b] (measured at 303 K) [23], plotted as a function of the volume fraction of water sorbed in the polymer. Values for the static permittivity of water and PTFE are also shown. The long dashed line represents a static permittivity (or dielectric constant) linear approximation. The short dashed line illustrates the different functional relationship between static permittivity and volume fraction of water for XL-pGMA-z compared to Nafion®. Uncertainty in the XL-pGMA-z data was taken as the standard deviation from the mean of three measurements.

3.4. Static permittivity

The static permittivity values for XL-pGMA-z are compared to results for Nafion® 117 in Fig. 4. We chose to use the static permittivity values obtained via regression using the single Debye relaxation model (see the SI for more details) for consistency. Comparing Figs. 2B and 4, however, reveals that the differences between the static permittivity values regressed using the model and the experimental data at the lowest frequency considered are relatively small with regard to the Nafion® 117 comparison. At similar water content, the XL-pGMA-z materials have a lower static permittivity compared that of Nafion® 117 membranes (where water content was adjusted by equilibrated Nafion® samples with different relative humidity environments) [23,71].

The long dashed line in Fig. 4 connects the static permittivity of PTFE with that for bulk pure water. The data for Nafion® samples are generally consistent with this trend. This observation has been used to approximate the static permittivity of other hydrated polymers based on knowledge of water content alone [13,21,22,35].

The short dashed line illustrates the increase in static permittivity for XL-pGMA-z with increasing water volume fraction. The XL-pGMA-z materials have lower static permittivity than Nafion® 117 and the linear approximation between PTFE and bulk pure water. This difference becomes more apparent as the water volume fraction increases. The data in Fig. 4 suggest that the functional relationship between hydrated polymer relative permittivity and water volume fraction may be affected by specific polymer chemistry, and relative permittivity property measurements may be needed to understand the behavior of different hydrated polymers.

The observed difference between the XL-pGMA-z and Nafion® 117 data, particularly at higher water volume fractions, is consistent with more non-freezable water in XL-pGMA-z compared to Nafion® 117 (Fig. 3). This situation could result in slower water dynamics in XL-pGMA-z compared to Nafion® 117. The phase-separated morphology of Nafion® 117 is reported to lead to water clustering around the sulfonate groups in that polymer [41], and those clusters can harbor freezable bulk or weakly bound water with faster dipole relaxations compared to the non-freezable water in XL-pGMA-z.

Table 3
Ion sorption coefficients for XL-pGMA-z and Nafion® 117 were measured after equilibrating the samples with 0.5 mol/L of NaCl. The hydrolysis time, z, refers to the length of time (in hours) that the XL-pGMA-z samples were immersed in 0.5 mol/L H_2SO_4 at 318 K. Measurements were made at 293 ± 1 K, and uncertainty was taken as the standard deviation from the mean of three measurements.

Polymer	Hydrolysis Time, z (h)	K_s	$\gamma_+^m\gamma_-^m$
XL-pGMA-z	0	0.012 ± 0.001	3025
	8	0.072 ± 0.006	84
	10	0.118 ± 0.007	31
	12	0.147 ± 0.001	20
Nafion®117	–	0.073 ± 0.003	1.1

3.5. Ion sorption

We measured ion sorption coefficients, K_s, and observed an increase in ion sorption as XL-pGMA-z water content increased (Table 3), which is consistent with results for many other hydrated polymers [4]. We compared the XL-pGMA-z ion sorption data to that for Nafion® 117. The water content of XL-pGMA-12 is similar to that for Nafion® 117, so it is reasonable to compare the ion sorption coefficients for these materials because K_s is highly sensitive to water content. We observed that ions were excluded from Nafion® 117 to a greater extent than XL-pGMA-12.

We combined the ion and water sorption data to analyze the sorption selectivity properties of the materials. The ion sorption coefficients for these materials are representative of the mobile salt sorption coefficient (i.e., the ions that can pass through the polymer as electrically neutral salts). Plotting the water/ion (or water/salt) sorption selectivity (i.e., K_w/K_s) versus the water sorption coefficient, K_w, provides insight into the ability of the polymer to exclude salt from sorbing into the polymer (an important metric for desalination membrane performance) at a given water content [13,91]. The sorption selectivity plays an important role in the desalination performance of a material, but details about rates of water and ion transport through the polymer, not discussed here, also influence the desalination performance of membrane materials [13,91]. In general, water/ion sorption selectivity decreased

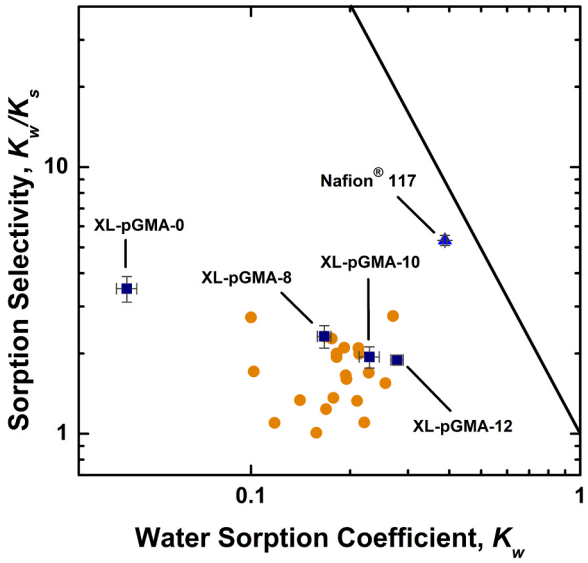

Fig. 5. Water/ion sorption selectivity, K_w/K_s as a function of K_w for XL-pGMA-z, Nafion® 117, and previously reported uncharged polymers (circles) [92]. The solid line represents a sorption selectivity trade-off frontier reported for desalination membranes [13,91].

as the XL-pGMA-z water content increased (Fig. 5), which is consistent with observations for other materials [4,13,91].

Nafion® 117 is more sorption selective compared to the XL-pGMA-z materials (Fig. 5). The presence of fixed charges on the Nafion® backbone contribute to ion exclusion via the Donnan exclusion mechanism [93]. As such, the higher water/ion sorption selectivity of charged Nafion® 117 compared to uncharged XL-pGMA-z is not surprising.

This influence of Donnan exclusion on ion sorption can be quantified using the measured ion sorption data to calculate the activity coefficients of ions sorbed in the membrane. In uncharged polymers studied using monovalent electrolytes, the mean ionic activity coefficient in the membrane phase, $\gamma_{\pm}^{m}$, can be related to the concentration of salt in the membrane, C_s^m, when the membrane is in equilibrium with an external salt solution of concentration C_s^s, and the mean ionic activity coefficient of the external solution, $\gamma_{\pm}^{s}$, as [94,95]:

$$(\gamma_{\pm}^{m})^2 = \gamma_{+}^{m}\gamma_{-}^{m} = \frac{(\gamma_{\pm}^{s})^2(C_s^s)^2}{(C_s^m)^2} = \left(\frac{\gamma_{\pm}^{s}}{K_s}\right)^2 \tag{9}$$

where γ_{+}^{m} and γ_{-}^{m} are the cation and anion activity coefficients in the membrane phase, respectively. The presence of negatively charged fixed charge groups in a cation exchange material, such as Nafion® 117, results in a similar relationship for the monovalent electrolyte ionic activity coefficients in the membrane phase [21]:

$$\gamma_{+}^{m}\gamma_{-}^{m} = \frac{(\gamma_{\pm}^{s})^2(C_s^s)^2}{C_{+}^{m}C_{-}^{m}} = \frac{(\gamma_{\pm}^{s})^2 C_s^s}{C_{+}^{m}K_s} \tag{10}$$

where C_{-}^{m} is the co-ion concentration in the membrane and C_{+}^{m} is the counter-ion concentration in the membrane.

In cation exchange materials, the concentration of co-ions is representative of the mobile salt concentration in the membrane phase, so $K_s \equiv C_{-}^{m}/C_s^s$, and $C_{+}^{m} = C_A^m + C_{-}^{m}$, where C_A^m is the concentration of fixed charges in the polymer [4,14]. The value of C_A^m for Nafion® 117 was determined to be 2.84 meq/cm^3 using the ion exchange capacity of Nafion® 117 [72] and water uptake data [21]. For 0.5 mol/L NaCl, the mean ionic activity coefficient in the solution phase, $\gamma_{\pm}^{s}$, was calculated to be 0.660 using the Pitzer model [96].

The ionic activity coefficients, calculated from the ion sorption data, suggest that Nafion® 117 is more thermodynamically ideal (i.e., the mean ionic activity coefficients are closer to unity) than XL-pGMA-z (Table 3). Additionally, XL-pGMA-z becomes more thermodynamically ideal as the water content of the polymer increases. These activity coefficients are consistent with the DSC data that suggest more freezable water exists in Nafion® 117 compared to XL-pGMA-z.

The activity coefficients can provide insight into the higher water/ion sorption selectivity of Nafion® 117 compared to XL-pGMA-z. The XL-pGMA-z polymers exclude salt via a dielectric mechanism that is described by Eq. (9) [18]. Unfavorable interactions between ions and the membrane phase result in exclusion of salt from the polymer, and this extent of exclusion increases as the ionic activity coefficients in the membrane phase increase and the water content of the polymer decreases.

The influence of dielectric exclusion on the overall ion sorption properties of Nafion® 117 is weak, in part, because the activity coefficients for Nafion® 117 are close to unity. As such, ion exclusion in Nafion® 117 is primarily driven by Donnan exclusion [19,93]. Therefore, it is reasonable that Nafion® 117 would have higher water/ion selectivity compared to XL-pGMA-z even though the relative permittivity of Nafion® 117 was greater than that of XL-pGMA-z at comparable water content.

3.6. Free energy of ion sorption

The ion sorption coefficient can be related to the free energy change associated with moving ions from the solution phase into the membrane phase, ΔW_s [13]:

$$K_s \equiv \frac{C_s^m}{C_s^s} = \exp\left[-\frac{\Delta W_s}{kT}\right] \tag{11}$$

where k is Boltzmann's constant, and T is absolute temperature [97]. In the simplest case, ΔW_s can be taken as the solvation energy barrier, which can be calculated using the electrostatic continuum-based approach proposed by Born [13,95,98,99]:

$$\Delta W_s = \frac{z_s^2 e^2}{8\pi\varepsilon_0 a_s}\left(\frac{1}{\varepsilon_m} - \frac{1}{\varepsilon_{sol}}\right) \tag{12}$$

where z_s is the ion charge number, e is the elementary charge, ε_0 is the permittivity of free space, a_s is the bare ion radius, ε_m is the relative permittivity of the membrane, and ε_{sol} is the dielectric constant of the external solution. The model assumes that both the solution and membrane can be treated as dielectric continua and that the ions are non-polarizable charged spheres [95,100,101].

Combining Eqs. (11) and (12) provides a means to estimate the significance of the difference between the static permittivity data for XL-pGMA-z and that calculated from the linear approximation discussed in regard to Fig. 4. For example, if the linear approximation was used to estimate the static permittivity of XL-pGMA-12, a value of 12.3 would be calculated based on the 0.278 ± 0.012 volume fraction of water in XL-pGMA-12 (Fig. 4). Eqs. (11) and (12) suggest that this value of the static permittivity would result in a value of K_s that is eight orders of magnitude larger than that calculated using the static permittivity of 5.3 measured for XL-pGMA-12.

The electrostatic theory-based Born model overestimates the solvation energy barrier for XL-pGMA-z likely as a result of the dielectric continuum assumptions for the polymer. The predicted values (calculated using Eq. (12)), however, are qualitatively consistent with experimental data (calculated using Eq. (11)), suggesting a decrease in the free energy barrier for ion sorption as polymer water content increases (Fig. 6). This qualitative agreement suggests that the static relative permittivity measurements captured part of the physics involved in the ion sorption process.

4. Conclusion

The relative permittivity of XL-pGMA-z increases with water content in a manner that is different from Nafion® 117. The relative permittivity values for XL-pGMA-z are also lower than that of Nafion® 117 at equivalent water content. This result may be due to the presence of

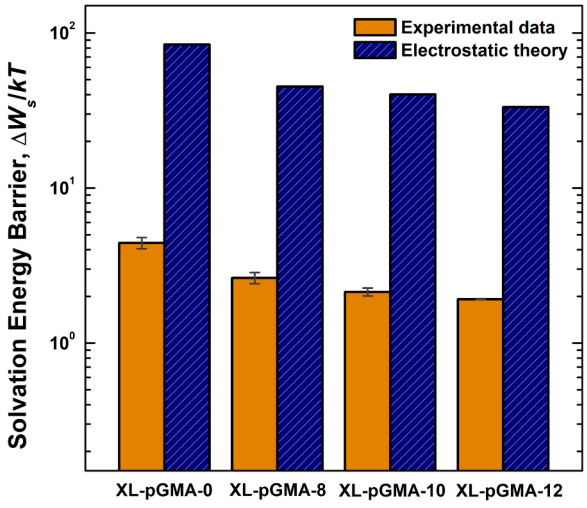

Fig. 6. Solvation energy barrier calculated (solid bars, experimental data) using measured sorption coefficients (Table 3) and Eq. (11), and calculated (striped bars, electrostatic theory) using static permittivity values (Fig. 4) and the Born model (Eq. (12)).

more extensive water-polymer hydrogen bonding in XL-pGMA-z that restricts water dipole dynamics to a greater extent than in Nafion® 117. As such, chemical details, not solely water content, appear to influence the relative permittivity properties of some hydrated polymers. These results suggest an opportunity to engineer membranes with low relative permittivity to minimize ion sorption in desalination-relevant materials. Measuring relative permittivity may provide insight into water dynamics and ion exclusion in a range of hydrated polymers.

Relative permittivity data for XL-pGMA-z was used to calculate the free energy barrier for ion sorption using the Born model. These values were compared to those values calculated using experimentally measured data. We observed qualitative agreement suggesting a decrease in the energy barrier as polymer water content increases, which is consistent with experimentally observed results. These results suggest that the static relatively permittivity measurements captured part of the physics that describes the ion sorption process and may provide insight into structure/property relationships between ion sorption and polymer chemistry. This understanding could inform future efforts to engineer highly water/ion sorption selective polymers for desalination membrane applications.

Acknowledgements

This material is based upon work supported in part by the National Science Foundation (NSF) Faculty Early Career Development (CAREER) Program (CBET-1752048) and the Oak Ridge Associated Universities (ORAU) Ralph E. Powe Junior Faculty Enhancement Award.

Appendix A. Supporting information

Supplementary data associated with this article can be found in the online version at doi:10.1016/j.memsci.2018.12.048.

References

[1] Y. Cohen, R. Semiat, A. Rahardianto, A perspective on reverse osmosis water desalination: Quest for sustainability, AIChE J. 63 (2017) 1771–1784.
[2] M. Elimelech, W.A. Phillip, The future of seawater desalination: energy, technology, and the environment, Science 333 (2011) 712–717.
[3] M.A. Shannon, P.W. Bohn, M. Elimelech, J.G. Georgiadis, B.J. Marinas, A.M. Mayes, Science and technology for water purification in the coming decades, Nature 452 (2008) 301–310.
[4] G.M. Geise, D.R. Paul, B.D. Freeman, Fundamental water and salt transport properties of polymeric materials, Prog. Polym. Sci. 39 (2014) 1–42.
[5] G.M. Geise, H.-S. Lee, D.J. Miller, B.D. Freeman, J.E. McGrath, D.R. Paul, Water purification by membranes: the role of polymer science, J. Polym. Sci. Part B: Polym. Phys. 48 (2010) 1685–1718.
[6] J. Kamcev, B.D. Freeman, Charged polymer membranes for environmental/energy applications, Annu. Rev. Chem. Biomol. Eng. 7 (2016) 111–133.
[7] C. Fritzmann, J. Löwenberg, T. Wintgens, T. Melin, State-of-the-art of reverse osmosis desalination, Desalination 216 (2007) 1–76.
[8] D.M. Stevens, J.Y. Shu, M. Reichert, A. Roy, Next-generation nanoporous materials: Progress and prospects for reverse osmosis and nanofiltration, Ind. Eng. Chem. Res. 56 (2017) 10526–10551.
[9] S. Surawanvijit, A. Rahardianto, Y. Cohen, An integrated approach for characterization of polyamide reverse osmosis membrane degradation due to exposure to free chlorine, J. Membr. Sci. 510 (2016) 164–173.
[10] T. Knoell, Municipal wastewater: chlorine's impact on the performance and properties of polyamide membranes, Ultrapure Water (2006) 24–31.
[11] J.R. Werber, A. Deshmukh, M. Elimelech, The critical need for increased selectivity, not increased water permeability, for desalination membranes, Environ. Sci. Technol. Lett. 3 (2016) 112–120.
[12] H.B. Park, J. Kamcev, L.M. Robeson, M. Elimelech, B.D. Freeman, Maximizing the right stuff: the trade-off between membrane permeability and selectivity, Science 356 (2017).
[13] H. Zhang, G.M. Geise, Modeling the water permeability and water/salt selectivity tradeoff in polymer membranes, J. Membr. Sci. 520 (2016) 790–800.
[14] G.M. Geise, L.P. Falcon, B.D. Freeman, D.R. Paul, Sodium chloride sorption in sulfonated polymers for membrane applications, J. Membr. Sci. 423 (2012) 195–208.
[15] L.F. Chen, Microwave Electronics: Measurement and Materials Characterization, Wiley, Hoboken, New Jersey, 2004.
[16] E. Glueckauf, On the mechanism of osmotic desalting with porous membranes, in: Proceedings of the First International Symposium on Water Desalination, 1967, pp. 143–150.
[17] J.E. Anderson, W. Pusch, The membrane/water partition coefficients of ions: electrostatic calculations of dielectric heterogeneity, Ber. Bunsenges. Phys. Chem. 80 (1976) 846–849.
[18] A.E. Yaroshchuk, Dielectric exclusion of ions from membranes, Adv. Colloid Interface Sci. 85 (2000) 193–230.
[19] A.E. Yaroshchuk, Non-steric mechanisms of nanofiltration: superposition of Donnan and dielectric exclusion, Sep. Purif. Technol. 22–23 (2001) 143–158.
[20] V. Freger, S. Bason, Characterization of ion transport in thin films using electrochemical impedance spectroscopy: I. principles and theory, J. Membr. Sci. 302 (2007) 1–9.
[21] J. Kamcev, M. Galizia, F.M. Benedetti, E.-S. Jang, D.R. Paul, B.D. Freeman, G.S. Manning, Partitioning of mobile ions between ion exchange polymers and aqueous salt solutions: importance of counter-ion condensation, Phys. Chem. Chem. Phys. 18 (2016) 6021–6031.
[22] J. Kamcev, D.R. Paul, G.S. Manning, B.D. Freeman, Predicting salt permeability coefficients in highly swollen, highly charged ion exchange membranes, ACS Appl. Mater. Interfaces 9 (2017) 4044–4056.
[23] S.J. Paddison, D.W. Reagor, T.A. Zawodzinski Jr, High frequency dielectric studies of hydrated Nafion®, J. Electroanal. Chem. 459 (1998) 91–97.
[24] Z. Lu, M. Lanagan, E. Manias, D.D. Macdonald, Two-port transmission line technique for dielectric property characterization of polymer electrolyte membranes, J. Phys. Chem. B 113 (2009) 13551–13559.
[25] K.A. Page, B.W. Rowe, K.A. Masser, A. Faraone, The effect of water content on chain dynamics in nafion membranes measured by neutron spin echo and dielectric spectroscopy, J. Polym. Sci. Part B: Polym. Phys. 52 (2014) 624–632.
[26] S. Paddison, G. Bender, T.A. Zawodzinski Jr, The microwave region of the dielectric spectrum of hydrated Nafion® and other sulfonated membranes, J. New Mater. Electrochem. Syst. 3 (2000) 293–302.
[27] H. Xu, J.K. Vij, V.J. McBrierty, Wide-band dielectric spectroscopy of hydrated poly (hydroxyethyl methacrylate), Polymer 35 (1994) 227–234.
[28] A. Kyritsis, P. Pissis, J. Grammatikakis, Dielectric relaxation spectroscopy in poly (hydroxyethyl acrylates)/water hydrogels, J. Polym. Sci. Part B: Polym. Phys. 33 (1995) 1737–1750.
[29] V.J. McBrierty, C.M. Keely, F.M. Coyle, H. Xu, J.K. Vij, Hydration and plasticization effects in cellulose acetate: molecular motion and relaxation, Faraday Discuss. 103 (1996) 255–268.
[30] A. Efligenir, P. Fievet, S. Déon, R. Salut, Characterization of the isolated active layer of a NF membrane by electrochemical impedance spectroscopy, J. Membr. Sci. 477 (2015) 172–182.
[31] G.E. Johnson, H.E. Bair, S. Matsuoka, E.W. Anderson, J.E. Scott, Water in Polymers, American Chemical Society, Washington, DC, 1980.
[32] A. De. La Rosa, L. Heux, J.Y. Cavaillé, Secondary relaxations in poly(allyl alcohol), PAA, and poly(vinyl alcohol), PVA. II. Dielectric relaxations compared with dielectric behaviour of amorphous dried and hydrated cellulose and dextran, Polymer 42 (2001) 5371–5379.
[33] S.J. Paddison, Proton conduction mechanisms at low degrees of hydration in sulfonic acid–based polymer electrolyte membranes, Annu. Rev. Mater. Res. 33 (2003) 289–319.
[34] Z. Lu, G. Polizos, D.D. Macdonald, E. Manias, State of water in perfluorosulfonic ionomer (Nafion® 117) proton exchange membranes, J. Electrochem. Soc. 155 (2008) B163–B171.
[35] J. Kamcev, D.R. Paul, B.D. Freeman, Ion activity coefficients in ion exchange polymers: applicability of Manning's counterion condensation theory, Macromolecules 48 (2015) 8011–8024.
[36] F. Müller-Plathe, Diffusion of water in swollen poly(vinyl alcohol) membranes studied by molecular dynamics simulation, J. Membr. Sci. 141 (1998) 147–154.
[37] Z. Lu, E. Manias, D.D. Macdonald, M. Lanagan, Dielectric relaxation in dimethyl sulfoxide/water mixtures studied by microwave dielectric relaxation spectroscopy, J. Phys. Chem. A 113 (2009) 12207–12214.
[38] J. Lou, T.A. Hatton, P.E. Laibinis, Effective dielectric properties of solvent mixtures at microwave frequencies, J. Phys. Chem. A 101 (1997) 5262–5268.
[39] P.B. Undre, P.W. Khirade, V.S. Rajenimbalkar, S.N. Helambe, S.C. Mehrotra, Dielectric relaxation in ethylene glycol - dimethyl sulfoxide mixtures as a function of composition and temperature, J. Korean Chem. Soc. 56 (2012) 416–423.
[40] P.W. Khirade, A. Chaudhari, J.B. Shinde, S.N. Helambe, S.C. Mehrotra, Static dielectric constant and relaxation time measurements on binary mixtures of dimethyl sulfoxide with ethanol, 2-ethoxyethanol, and propan-1-ol at 293, 303, 313, and 323 K, J. Chem. Eng. Data 44 (1999) 879–881.
[41] K.A. Mauritz, R.B. Moore, State of understanding of Nafion®, Chem. Rev. 104 (2004) 4535–4586.
[42] N.V. Tsarevsky, W. Jakubowski, Atom transfer radical polymerization of functional monomers employing Cu-based catalysts at low concentration: polymerization of glycidyl methacrylate, J. Polym. Sci. Part A: Polym. Chem. 49 (2011) 918–925.
[43] R.G. Geyer, J. Krupka, Microwave dielectric properties of anisotropic materials at cryogenic temperatures, IEEE Trans. Instrum. Meas. 44 (1995) 329–331.
[44] T.A. Zawodzinski, T.E. Springer, J. Davey, R. Jestel, C. Lopez, J. Valerio, S. Gottesfeld, A comparative study of water uptake by and transport through ionomeric fuel cell membranes, J. Electrochem. Soc. 140 (1993) 1981–1985.
[45] T.A. Zawodzinski, M. Neeman, L.O. Sillerud, S. Gottesfeld, Determination of water diffusion coefficients in perfluorosulfonate ionomeric membranes, J. Phys. Chem. 95 (1991) 6040–6044.
[46] G.M. Geise, C.L. Willis, C.M. Doherty, A.J. Hill, T.J. Bastow, J. Ford, K.I. Winey, B.D. Freeman, D.R. Paul, Characterization of aluminum-neutralized sulfonated styrenic pentablock copolymer films, Ind. Eng. Chem. Res. 52 (2013) 1056–1068.
[47] G.M. Geise, M.A. Hickner, B.E. Logan, Ionic resistance and permselectivity

tradeoffs in anion exchange membranes, ACS Appl. Mater. Interfaces 5 (2013) 10294–10301.
[48] G.M. Geise, B.D. Freeman, D.R. Paul, Sodium chloride diffusion in sulfonated polymers for membrane applications, J. Membr. Sci. 427 (2013) 186–196.
[49] K. Chang, T. Xue, G.M. Geise, Increasing salt size selectivity in low water content polymers via polymer backbone dynamics, J. Membr. Sci. 552 (2018) 43–50.
[50] J. Rumble, CRC Handbook of Chemistry and Physics, 98th ed., CRC Press LLC, Boca Raton, Florida, 2017.
[51] H. Luo, J. Aboki, Y. Ji, R. Guo, G.M. Geise, Water and salt transport properties of triptycene-containing sulfonated polysulfone materials for desalination membrane applications, ACS Appl. Mater. Interfaces 10 (2018) 4102–4112.
[52] D. Halliday, R. Resnick, J. Walker, Fundamentals of Physics, 7th ed., Wiley, Hoboken, New Jersey, 2005.
[53] H. Ju, A.C. Sagle, B.D. Freeman, J.I. Mardel, A.J. Hill, Characterization of sodium chloride and water transport in crosslinked poly(ethylene oxide) hydrogels, J. Membr. Sci. 358 (2010) 131–141.
[54] C.L. Yaws, R.W. Pike, Thermophysical Properties of Chemicals and Hydrocarbons, William Andrew, Norwich, New York, 2009.
[55] G.M. Geise, B.D. Freeman, D.R. Paul, Characterization of a sulfonated pentablock copolymer for desalination applications, Polymer 51 (2010) 5815–5822.
[56] A.M. Nicolson, G.F. Ross, Measurement of the intrinsic properties of materials by time-domain techniques, IEEE Trans. Instrum. Meas. 19 (1970) 377–382.
[57] W.B. Weir, Automatic measurement of complex dielectric constant and permeability at microwave frequencies, Proc. IEEE 62 (1974) 33–36.
[58] Keysight Technologies, How to Perform a Waveguide Calibration with Opt.001, ⟨http://na.support.keysight.com/materials/help/WebHelp/Opt.001_How_to_Perform_a_Waveguide_Calibration.htm⟩ (Accessed 13 June 2018).
[59] G. Smith, A.P. Duffy, J. Shen, C.J. Olliff, Dielectric relaxation spectroscopy and some applications in the pharmaceutical sciences, J. Pharm. Sci. 84 (1995) 1029–1044.
[60] P.G. Bartley, S.B. Begley, A new technique for the determination of the complex permittivity and permeability of materials, in: Proceedings of IEEE Instrumentation & Measurement Technology Conference, 2010, pp. 54–57.
[61] D.M. Kerns, R.W. Beatty, Basic Theory of Waveguide Junctions and Introductory Microwave Network Analysis, 1st ed., Pergamon Press, Oxford, New York, 1967.
[62] J. Baker-Jarvis, E.J. Vanzura, W.A. Kissick, Improved technique for determining complex permittivity with the transmission/reflection method, IEEE Trans. Microw. Theory Tech. 38 (1990) 1096–1103.
[63] Keysight Technologies, N1500A Materials Measurement Suite, ⟨http://literature.cdn.keysight.com/litweb/pdf/5992-0263EN.pdf⟩ (Accessed 13 June 2018).
[64] P.I. Somlo, A convenient self-checking method for the automated microwave measurement of mu and epsilon, IEEE Trans. Instrum. Meas. 42 (1993) 213–216.
[65] N. Qaddoumi, S. Ganchev, R. Zoughi, Microwave diagnosis of low-density fiberglass composites with resin binder, Res. Nondestruct. Eval. 8 (1996) 177–188.
[66] K.J. Bois, L.F. Handjojo, A.D. Benally, K. Mubarak, R. Zoughi, Dielectric plug-loaded two-port transmission line measurement technique for dielectric property characterization of granular and liquid materials, IEEE Trans. Instrum. Meas. 48 (1999) 1141–1148.
[67] TA Instruments, Purge Gas Recommendations for use in Modulated DSC®, ⟨http://www.tainstruments.com/pdf/literature/TN44.pdf⟩ (Accessed 13 June 2018).
[68] E.L. Cussler, Diffusion: Mass Transfer in Fluid Systems, 3rd ed., Cambridge University Press, Cambridge, New York, 2009.
[69] J. Crank, The Mathematics of Diffusion, 2nd ed., Clarendon Press, Oxford, New York, 1975.
[70] J.S. Mackie, P. Meares, The diffusion of electrolytes in a cation-exchange resin membrane I. Theoretical, Prioc. R. Soc. Lond. Ser. A Math. Phys. Sci. 232 (1955) 498–509.
[71] Z. Lu, State of Water in Perfluorosulfonic Acid Membranes Studied by Microwave Dielectric Relaxation Spectroscopy (Ph.D. thesis), Department of Materials Science and Engineering, The Pennsylvania State University, University Park, Pennsylvania, 2006.
[72] Alfa Aesar by Thermo Fisher Scientific, Nafion® N-117 membrane, 0.180 mm thick, ≥ 0.90 meq/g exchange capacity, ⟨https://www.alfa.com/en/catalog/042180/⟩ (Accessed 13 June 2018).
[73] Keysight Technologies, Sample and Sample Holder Considerations (Opt.001), ⟨http://na.support.keysight.com/materials/help/WebHelp/Opt.001_Sample_and_Sample_Holder_Considerations.htm⟩ - efd32146 (Accessed 12 June 2018).
[74] Keysight Technologies, Basics of Measuring the Dielectric Properties of Materials, ⟨https://literature.cdn.keysight.com/litweb/pdf/5989-2589EN.pdf?Id=670519⟩ (Accessed 12 June 2018).
[75] Keysight Technologies, Opt.001 Sample Thickness Calculator, ⟨http://na.support.keysight.com/materials/help/WebHelp/Opt.001_Sample_Thickness_Calculator.htm⟩ (Accessed 12 June 2018).
[76] P. Debye, Polar Molecules, Dover, New York, 1929.
[77] W.J. Ellison, K. Lamkaouchi, J.M. Moreau, Water: A dielectric reference, J. Mol. Liq. 68 (1996) 171–279.
[78] K.-D. Kreuer, S.J. Paddison, E. Spohr, M. Schuster, Transport in proton conductors for fuel-cell applications: simulations, elementary reactions, and phenomenology, Chem. Rev. 104 (2004) 4637–4678.
[79] J.A. Elliott, S.J. Paddison, Modelling of morphology and proton transport in PFSA membranes, Phys. Chem. Chem. Phys. 9 (2007) 2602–2618.
[80] TA Instruments, Thermal Analysis to Determine Various Forms of Water Present in Hydrogels, ⟨http://www.tainstruments.com/pdf/literature/TA384.pdf⟩ (Accessed 12 June 2018).
[81] F.X. Quinn, E. Kampff, G. Smyth, V.J. McBrierty, Water in hydrogels. 1. A study of water in poly(N-vinyl-2-pyrrolidone/methyl methacrylate) copolymer, Macromolecules 21 (1988) 3191–3198.
[82] R.M. Hodge, T.J. Bastow, G.H. Edward, G.P. Simon, A.J. Hill, Free volume and the mechanism of plasticization in water-swollen poly(vinyl alcohol), Macromolecules 29 (1996) 8137–8143.
[83] H. Yoshida, Y. Miura, Behavior of water in perfluorinated ionomer membranes containing various monovalent cations, J. Membr. Sci. 68 (1992) 1–10.
[84] N. Shinyashiki, M. Shimomura, T. Ushiyama, T. Miyagawa, S. Yagihara, Dynamics of water in partially crystallized polymer/water mixtures studied by dielectric spectroscopy, J. Phys. Chem. B 111 (2007) 10079–10087.
[85] T. Shimoaka, C. Wakai, T. Sakabe, S. Yamazaki, T. Hasegawa, Hydration structure of strongly bound water on the sulfonic acid group in a Nafion membrane studied by infrared spectroscopy and quantum chemical calculation, Phys. Chem. Chem. Phys. 17 (2015) 8843–8849.
[86] N.J. Bunce, S.J. Sondheimer, C.A. Fyfe, Proton NMR method for the quantitative determination of the water content of the polymeric fluorosulfonic acid Nafion-H, Macromolecules 19 (1986) 333–339.
[87] Y.S. Kim, L. Dong, M.A. Hickner, T.E. Glass, V. Webb, J.E. McGrath, State of water in disulfonated poly(arylene ether sulfone) copolymers and a perfluorosulfonic acid copolymer (Nafion) and its effect on physical and electrochemical properties, Macromolecules 36 (2003) 6281–6285.
[88] E.E. Boakye, H.L. Yeager, Water sorption and ionic diffusion in short side chain perfluorosulfonate ionomer membranes, J. Membr. Sci. 69 (1992) 155–167.
[89] W.A.P. Luck, The Influence of Ions on Water Structure and on Aqueous Systems, Springer, Boston, MA, 1985.
[90] K.D. Kreuer, On the development of proton conducting polymer membranes for hydrogen and methanol fuel cells, J. Membr. Sci. 185 (2001) 29–39.
[91] G.M. Geise, H.B. Park, A.C. Sagle, B.D. Freeman, J.E. McGrath, Water permeability and water/salt selectivity tradeoff in polymers for desalination, J. Membr. Sci. 369 (2011) 130–138.
[92] H. Yasuda, C.E. Lamaze, L.D. Ikenberry, Permeability of solutes through hydrated polymer membranes. Part I. Diffusion of sodium chloride, Die Makromol. Chem. 118 (1968) 19–35.
[93] F.G. Helfferich, Ion Exchange, McGraw-Hill, New York, 1962.
[94] J.G. Wijmans, R.W. Baker, The solution-diffusion model: a review, J. Membr. Sci. 107 (1995) 1–21.
[95] Y. Ji, H. Luo, G.M. Geise, Specific co-ion sorption and diffusion properties influence membrane permselectivity, J. Membr. Sci. 563 (2018) 492–504.
[96] K.S. Pitzer, J.C. Peiper, R.H. Busey, Thermodynamic properties of aqueous sodium chloride solutions, J. Phys. Chem. Ref. Data 13 (1984) 1–102.
[97] J.M. Prausnitz, R.N. Lichtenthaler, E.Gd Azevedo, Molecular Thermodynamics of Fluid-Phase Equilibria, 2nd ed., Prentice-Hall, Englewood Cliffs, New Jersey, 1986.
[98] W.R. Bowen, J.S. Welfoot, P.M. Williams, Linearized transport model for nanofiltration: development and assessment, AIChE J. 48 (2002) 760–773.
[99] M. Born, Volumen und hydratationswärme der ionen, Z. Phys. 1 (1920) 45–48.
[100] A. Parsegian, Energy of an ion crossing a low dielectric membrane: solutions to four relevant electrostatic problems, Nature 221 (1969) 844.
[101] J.R. Bontha, P.N. Pintauro, Prediction of ion solvation free energies in a polarizable dielectric continuum, J. Phys. Chem. 96 (1992) 7778–7782.